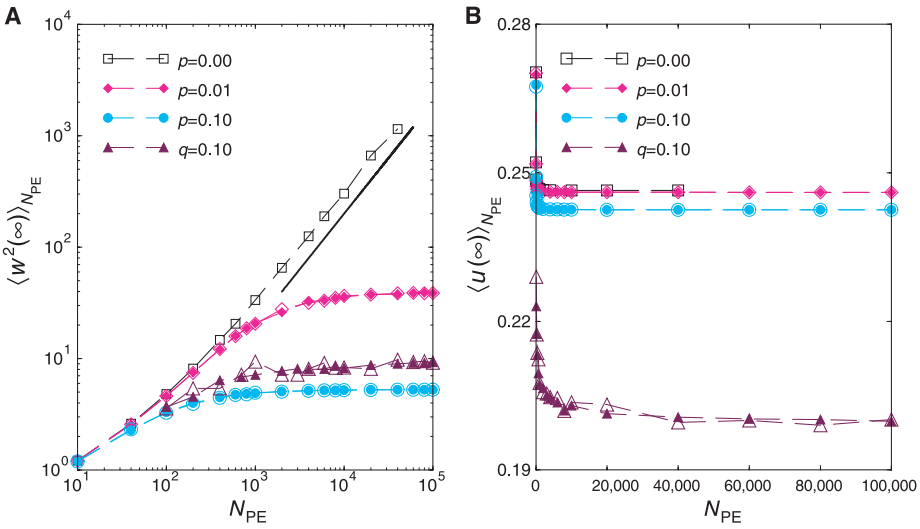

Fig. 3. (**A**) Average steady-state width of the virtual time horizon for various values of p for the one-site-per-PE PDES scheme. In addition to ensemble averages over 10 realizations of the random links (solid symbols), a single realization is also shown (the same open symbols). The solid straight line represents the asymptotic one-dimensional KPZ power-law divergence with roughness exponent $\alpha = 1/2$ for the $p = 0$ case. Note the log-log scales. The $q = 0.10$ data set corresponds to the case when only 10% of the PEs have random links and those are checked at every step. (**B**) The steady-state utilization (fraction of nonidling PEs) for the same cases as in (A).

about 5.25 (Fig. 3A) while $\langle u(\infty)\rangle_{N_{PE}}$ is reduced by only about 1.6% (Fig. 3B). One can also observe the clear self-averaging property for both global observables, the width and the utilization (Fig. 3). From a broader statistical physics viewpoint, one can ask whether a small, nonzero fraction q of the PEs with random links (checked, e.g., at every step) is sufficient to control the width. Although this choice clearly weakens load balancing and the utilization (Fig. 3B), our results in Fig. 3A and recent work on the closely related XY-model on a small-world network (*25*) suggest that a finite width is achieved. There is growing evidence that systems without inherent frustration exhibit mean-field characteristics when the original short-range interaction topology is modified to a small-world network (*23, 25–27*).

The generalization when random links are added to a higher-dimensional underlying regular lattice is clear: Because the one-dimensional case with random links is governed by the mean-field equation, in higher dimensions it will be even more so [i.e., the critical dimension (*18*) of the model with random links is less than 1]. The generalization for the many-sites-per-PE case also follows from universality arguments: Without the random connections, there is an additional fast-roughening phase for early times when the evolution of the time horizon corresponds to random deposition (*18*). Subsequently, it will cross over to the KPZ growth regime and finally saturate. With many sites per PE, the typically desired and efficient way of implementing PDES (*7, 15*), the saturation value of the width can become extremely large. This underscores the importance of implementing the additional synchronizations through random links to suppress the roughness of the time horizon.

References and Notes

1. R. Fujimoto, *Commun. ACM* **33**, 30 (1990).
2. D. M. Nicol, R. M. Fujimoto, *Ann. Oper. Res.* **53**, 249 (1994).
3. B. D. Lubachevsky, *Bell Labs Tech. J.* **5** (April–June), 134 (2000).
4. A. G. Greenberg *et al.*, in *Proceedings of the 8th Workshop on Parallel and Distributed Simulation (PADS'94), Edinburgh, UK, 1994* (Society for Computer Simulation, San Diego, CA, 1994), pp. 187–194.
5. E. Deelman, B. K. Szymanski, T. Caraco, in *Proceedings of the 28th Winter Simulation Conference* (Association for Computing Machinery, New York, 1996), pp. 1191–1198.
6. D. M. Nicol, in *Proceedings of the SCS Multiconference on Distributed Simulation* (Society for Computer Simulation, San Diego, CA, 1988), vol. 19, pp. 141–146.
7. G. Korniss, M. A. Novotny, P. A. Rikvold, *J. Comput. Phys.* **153**, 488 (1999).
8. G. Korniss, C. J. White, P. A. Rikvold, M. A. Novotny, *Phys. Rev. E* **63**, 016120 (2001).
9. P. M. A. Sloot, B. J. Overeinder, A. Schoneveld, *Comput. Phys. Commun.* **142**, 76 (2001).
10. D. R. Jefferson, *ACM Trans. Prog. Lang. Syst.* **7**, 404 (1985).
11. P. Bak, C. Tang, K. Wiesenfeld, *Phys. Rev. Lett.* **59**, 381 (1987).
12. A. G. Greenberg, S. Shenker, A. L. Stolyar, *Performance Eval. Rev.* **24**, 91 (1996).
13. K. M. Chandy, J. Misra, *Commun. ACM* **24**, 198 (1981).
14. B. D. Lubachevsky, *Complex Syst.* **1**, 1099 (1987).
15. ———, *J. Comput. Phys.* **75**, 103 (1988).
16. G. Korniss, Z. Toroczkai, M. A. Novotny, P. A. Rikvold, *Phys. Rev. Lett.* **84**, 1351 (2000).
17. G. Korniss, M. A. Novotny, Z. Toroczkai, P. A. Rikvold, in *Computer Simulation Studies in Condensed Matter Physics XIII*, D. P. Landau, S. P. Lewis, H.-B. Schüttler, Eds., vol. 86 of *Springer Proceedings in Physics* (Springer-Verlag, Berlin, 2001), pp. 183–188.
18. A.-L. Barabási, H. E. Stanley, *Fractal Concepts in Surface Growth* (Cambridge Univ. Press, Cambridge, 1995).
19. T. Halpin-Healy, Y.-C. Zhang, *Phys. Rep.* **254**, 215 (1995).
20. M. Kardar, G. Parisi, Y.-C. Zhang, *Phys. Rev. Lett.* **56**, 889 (1986).
21. Z. Toroczkai, G. Korniss, S. Das Sarma, R. K. P. Zia, *Phys. Rev. E* **62**, 276 (2000).
22. D. J. Watts, S. H. Strogatz, *Nature* **393**, 440 (1998).
23. M. E. J. Newman, *J. Stat. Phys.* **101**, 819 (2000).
24. Here we define the Fourier transform of the surface fluctuations as
$$\tilde{\tau}_k = \sum_{j=1}^{N_{PE}} [\exp(-ikj)](\tau_j - \bar{\tau})$$
where $k = 2\pi n/N_{PE}$ and $n = 0, 1, 2, \ldots, N_{PE} - 1$.
25. B. J. Kim *et al.*, *Phys. Rev. E* **64**, 056135 (2001).
26. A. Barrat, M. Weigt, *Eur. Phys. J. B* **13**, 547 (2000).
27. M. Gitterman, *J. Phys. A* **33**, 8373 (2000).

28. We thank G. Istrate and Z. Rácz for discussions. Supported by NSF grants DMR-0113049 and DMR-9981815, Research Corporation grant RI0761, and U.S. Department of Energy grant W-7405-ENG-36 (Z.T.).

15 October 2002; accepted 12 December 2002

A Gate-Controlled Bidirectional Spin Filter Using Quantum Coherence

J. A. Folk,[1,2]* R. M. Potok,[1] C. M. Marcus,[1]* V. Umansky[3]

We demonstrate a quantum coherent electron spin filter by directly measuring the spin polarization of emitted current. The spin filter consists of an open quantum dot in an in-plane magnetic field; the in-plane field gives the two spin directions different Fermi wavelengths resulting in spin-dependent quantum interference of transport through the device. The gate voltage is used to select the preferentially transmitted spin, thus setting the polarity of the filter. This provides a fully electrical method for the creation and detection of spin-polarized currents. Polarizations of emitted current as high as 70% for both spin directions (either aligned or anti-aligned with the external field) are observed.

The ability to controllably generate and detect electron spin in mesoscopic systems is important for the field of spintronics and is also a powerful tool for investigating basic properties of spin in coherent electronic systems. The development of tunable spin filters

has, therefore, been the goal of many research programs over the last several years.

Some notable successes have already been achieved: spin polarizations of ~15% from all-metal devices using ferromagnetic spin injectors (*1*, *2*) and spin injection from ferromagnetic semiconductors into normal semiconductors with polarizations of up to 90% (*3*, *4*) have been reported. We have sought to realize a highly selective spin filter in a clean, quantum coherent system and to use a gate voltage to control the polarization of the filter without needing to reverse externally applied magnetic fields.

Narrow constrictions called quantum point contacts (QPCs) in a two-dimensional electron gas (2DEG) have recently been shown to act as spin filters in magnetic fields of several tesla, due either to Zeeman splitting when the field is in the plane of the 2DEG or to spin-resolved Landau quantization when the field is perpendicular to the 2DEG (*5*, *6*). The filtering properties of point contacts can be turned on and off by adjusting the voltage on electrostatic gates. Fast gating techniques developed in conventional microelectronics can then be used to produce rapidly activated filters without having to change the applied magnetic fields. A disadvantage of a QPC spin filter, however, is that its polarity cannot be reversed without reversing the external field (*6*).

Our spin filter consists of a small (~100 electron) lateral quantum dot in a GaAs/AlGaAs heterostructure (Fig. 1A). At low temperatures, such dots are known to exhibit universal conductance fluctuations (UCF) (*7*) resulting from quantum interference of coherent transport paths. In an in-plane magnetic field, the different Fermi wavelengths of spin-up and spin-down electrons lead to different interference patterns for opposite spin directions. The dot may, therefore, be tuned with the use of gate voltages to configurations where the transmission of one or the other spin is strongly suppressed by destructive interference, thus forming a tunable spin filter.

Spin filtering properties were measured in a polarizer-analyzer geometry, where the spin polarization of current emitted from the dot (the polarizer) in an in-plane field, $B_{\|}$, was detected using a QPC at $0.5e^2/h$ (the analyzer) (*6*). The polarizer and analyzer elements were coupled by transverse focusing with the use of a small perpendicular magnetic field, $B_{\perp}$ (*6*, *8*). With constant current flowing between the emitter and base regions, focusing peaks (i.e., peaks in the collector-base voltage, V_c) were observed at fields where the distance between the emitter and collector was an integer multiple of the cyclotron diameter $2m^*v_F/eB_{\perp}$ (m^* is effective electron mass, v_F is Fermi velocity). Data are presented for the second focusing peak (at ~160 mT, Fig. 1B), with others showing consistent behavior.

In an in-plane field, the height of a focusing peak reflects the degree of spin polarization of the emitted current whenever the detector QPC conductance, g_c, is in a spin-selective regime, $g_c < e^2/h$ (*6*). This occurs because the collector does not sink current, so a voltage $V_c = I_c/g_c$ develops between collector and base in response to current injected into the collector region, $I_c = \alpha(I_{\uparrow e}T_{\uparrow c} + I_{\downarrow e}T_{\downarrow c})$. (The efficiency parameter α, where $0 < \alpha < 1$, accounts for spin-independent imperfections in the focusing process.) With emitter current, $I_e = I_{\uparrow e} + I_{\downarrow e}$, held fixed, the focusing signal then only depends on the emitter polarization, $P_e = (I_{\uparrow e} - I_{\downarrow e})/(I_{\uparrow e} + I_{\downarrow e})$, and collector sensitivity, $P_c = (T_{\uparrow c} - T_{\downarrow c})/(T_{\uparrow c} + T_{\downarrow c})$ (*6*)

$$V_c = \alpha(h/2e^2)I_e(1 + P_eP_c) \qquad (1)$$

The device was fabricated on a high-mobility GaAs/AlGaAs 2DEG using depletion gates on the surface of the wafer. The high mobility of this sample ($\mu = 5.5 \times 10^6$ cm^2/Vs, limited mostly by remote impurity scattering) was necessary to observe clear focusing peaks. This mobility and an electron density of 1.3×10^{11} cm^{-2} yield a mean free path of 45 μm and a Fermi velocity of $v_F = 2 \times 10^7$ cm/s, consistent with the observed spacing between focusing peaks of ~ 80 mT. Measurements were performed in a dilution refrigerator with a base electron temperature of 70 mK. A standard superconducting solenoid was used to generate the in-plane field, and an independent superconducting coil was used to generate perpendicular magnetic fields.

Focusing peaks were measured at $B_{\|} = 6$ T with a spin-sensitive ($g_c = 0.5e^2/h$) collector (Fig. 1, C and D). In Fig. 1C, two of the gates forming the dot were undepleted, making the emitter a single QPC set at $2e^2/h$. In this case, one does not expect spin polarization in the emitter current to fluctuate with plunger gate voltage. As anticipated, the height of the focusing peak remains constant. In contrast, when all gates were depleted, a dot was formed at the emitter with both leads of the dot set to $2e^2/h$ (Fig. 1D). In this case, quantum interference within the dot (also the

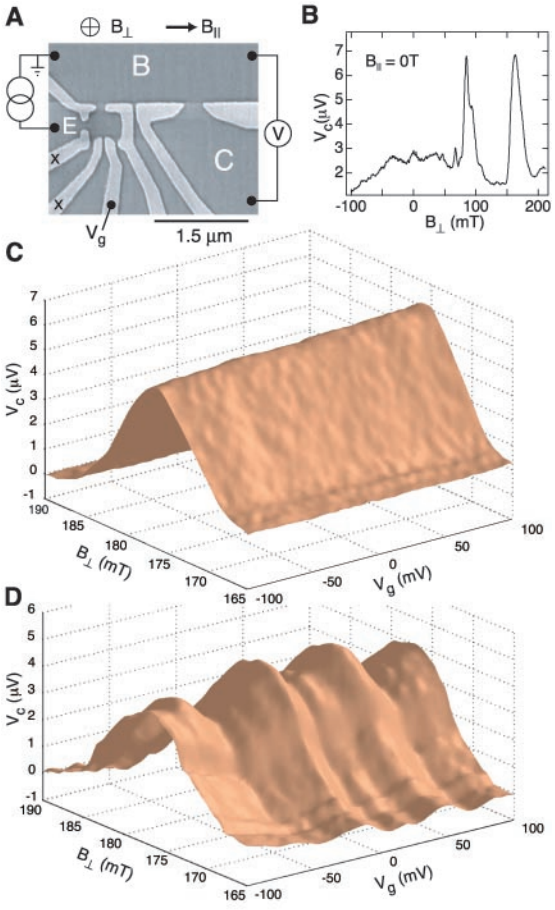

Fig. 1. (**A**) Micrograph and circuit showing the polarizer-analyzer configuration used in the experiment. The emitter, labeled "E," can be formed into either a quantum dot or a point contact. The collector, "C," is a single point contact. Electrons are focused from emitter to collector through the base region, "B," using a small perpendicular magnetic field. Gates marked with "x" are left undepleted when the emitter is operated as a point contact. (**B**) Base-collector voltage (V_c) showing two focusing peaks. (**C** and **D**) Focusing peak as a function of plunger gate voltage (V_g) with spin-selective collector ($g_c = 0.5e^2/h$). Small background Hall voltage is subtracted off. (C) Emitter is single QPC at $2e^2/h$. (D) Emitter is quantum dot, with both leads at $2e^2/h$. Fluctuations in focusing are not sensitive to conductance fluctuations, because the current is held fixed. Rather, focusing peak fluctuations reflect fluctuations in spin polarization of emitted current.

[1]Department of Physics, Harvard University, Cambridge, MA 02138, USA. [2]Department of Physics, Stanford University, Stanford, CA 94305, USA. [3]Braun Center for Submicron Research, Weizmann Institute of Science, Rehovot 76100, Israel.

*To whom correspondence should be addressed. E-mail: jfolk@stanford.edu (J.A.F.); marcus@harvard.edu (C.M.M.)

source of conductance fluctuations) is expected to give rise to fluctuations in the spin polarization of the emitted current, even though the leads of the dot are not polarizing. These mesoscopic fluctuations of spin current polarization appear as fluctuations in the focusing peak height. We emphasize that the total emitted current was held at a fixed level using a current bias and did not fluctuate as the dot conductance changed. The focusing peak position also does not change as a function of plunger voltage, allowing peak height fluctuations to be measured at fixed $B_\perp$.

Figure 2A shows focusing peak heights at $B_\parallel$ = 6 T with a spin-selective collector (g_c = $0.5e^2/h$) for the cases of either a dot or a QPC as emitter. With the emitter configured as a single QPC on the $2e^2/h$ plateau (black curve), the focusing peak shows only weak fluctuations as a function of a plunger gate voltage. This is the control case of unpolarized emission, P_e = 0. When the dot is fully formed (red curve), fluctuations in the focusing peak height extend above and below the unpolarized curve, demonstrating that the polarization P_e shows mesoscopic fluctuations around zero. That is, the polarization may be either aligned or antialigned with the applied field, depending on the plunger gate voltage.

Focusing peak heights (normalized by their averages) are shown (Fig. 2B) under various polarization conditions of emitter and collector. The red curve shows bidirectional spin current fluctuations when the dot was formed and the collector was spin selective (g_c = $0.5e^2/h$) at $B_\parallel$ = 6 T. Removing the spin sensitivity of the collector by setting g_c to $2e^2/h$ caused the fluctuations to disappear (green curve). At $B_\parallel$ = 0, fluctuations were also absent, irrespective of g_c (blue curve). In all cases, fluctuations in conductance remained large (Fig. 2C), verifying that the spin-dependent focusing peak fluctuations were not due to UCF.

In order to extract quantitatively the spin polarization of emitted current (P_e), we must first measure the collector sensitivity (P_c), which will be less than one due to finite temperature and mode mixing. To find P_c, we configure the emitter as a single QPC and compare focusing peak heights at $B_\parallel$ = 6T and g_c = $0.5e^2/h$ for the cases g_e = e^2/h and g_e = $2e^2/h$. Fully polarized emission and detection would give peak heights differing by a factor of two (Eq. 1), but we found a factor of 1.5, indicating incomplete polarization (Fig. 3A, inset). Assuming the point contacts have equal polarization gives a value $P_c = P_e = \sqrt{1.5 - 1} \sim 0.7$. The rather poor quality of the collector QPC relative to the emitter (Fig. 3B, right inset) suggests that P_c is, in fact, less than P_e. Using the value P_c = 0.7 to convert focusing signals to emitter polarizations in Fig. 2A and Fig. 4 therefore provides conservative estimates of P_e.

Figure 3 shows fluctuations of emitter polarization as the conductance of the exit QPC of the dot in the emitter (Fig. 3B, left inset) is reduced below $2e^2/h$, with the entrance QPC held at $2e^2/h$. The upward trend in polarization as the exit QPC is closed shows that a dot that can generate polarizations in both directions when both leads are open will generate only a single direction of polarization, passing the lower energy spin, when the exit lead is set well below $2e^2/h$. A similar effect, where one direction of polarization becomes favored, is observed when either entrance or exit QPC, or both, is reduced into the tunneling regime. This may complicate the use of Coulomb-blockaded quantum dots as bidirectional spin filters.

Finally, we examined the statistics of the spin polarization of current emitted from the dot, sampled over an ensemble of dot shapes (Fig. 4) (*9*). Roughly 200 independent shapes were used to generate the histogram (Fig. 4A). For comparison, also shown is a simple random matrix theory calculation, treating the case of Zeeman energy greatly exceeding the dot level

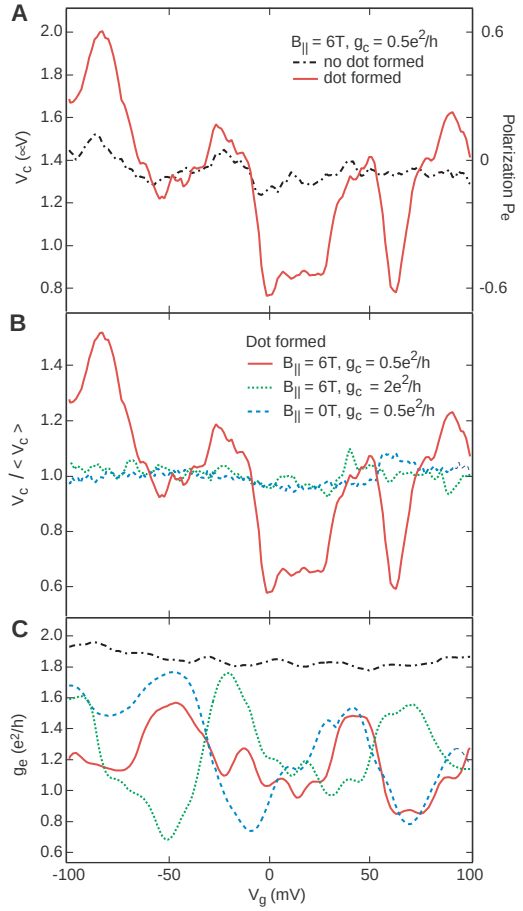

Fig. 2. (**A**) Focusing peak height at $B_\parallel$ = 6 T with spin-selective collector, g_c = $0.5e^2/h$, comparing emitter as point contact at $2e^2/h$ (black curve) and emitter as quantum dot with both leads at $2e^2/h$ (red curve). (**B**) Comparison of normalized focusing peak height fluctuations as a function of V_g at $B_\parallel$ = 6 T for a spin-selective collector, g_c = $0.5e^2/h$ (red curve), at $B_\parallel$ = 6 T for an unpolarized collector, g_c = $2e^2/h$ (green curve), and at $B_\parallel$ = 0 with g_c = $0.5e^2/h$ (blue curve). Significant fluctuations of collector voltage are seen only when the collector is spin-sensitive (red curve). Dividing by average peak height, $|V_c|$, normalizes for changes in focusing efficiency, α. (**C**) Conductance of the emitter, g_e, for the cases described above: a spin-polarized collector at $B_\parallel$ = 6 T (red curve), an unpolarized collector at $B_\parallel$ = 6 T (green curve), at $B_\parallel$ = 0 with g_c = $0.5e^2/h$ (blue curve), and for an unformed dot with emitter point contact at $2e^2/h$ with $B_\parallel$ = 6 T (black curve).

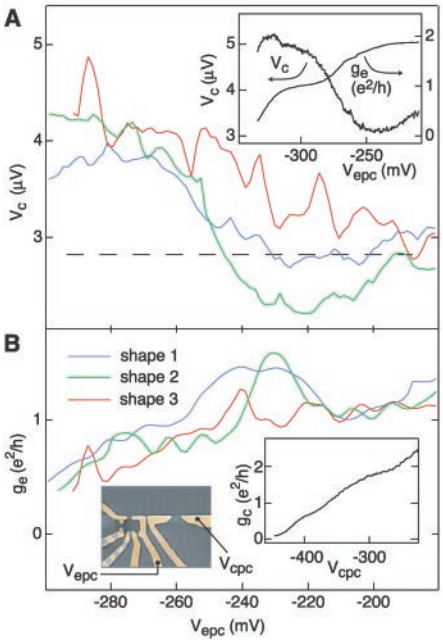

Fig. 3. (**A**) Focusing peak heights at $B_\parallel$ = 6 T for three different dot shapes as the exit point contact of the emitter dot is reduced from $2e^2/h$ (at $V_{epc} \sim -220$ mV) to $\sim 1e^2/h$ (at $V_{epc} \sim -300$ mV). The rising of the average focusing signal above the unpolarized level (dashed line) as the exit point contact is reduced below $2e^2/h$ demonstrates that spin currents of only a single polarization direction are possible when the exit point contact is spin selective. (Inset) Emitter conductance, showing clear plateaus and corresponding focusing peak height when emitter is a single QPC. (**B**) Conductances of the emitter dot as the exit point contact is swept, for the three shapes shown above. (Left inset) Micrograph indicating gates swept. (Right inset) Collector point contact conductance, showing relatively weak plateaus.

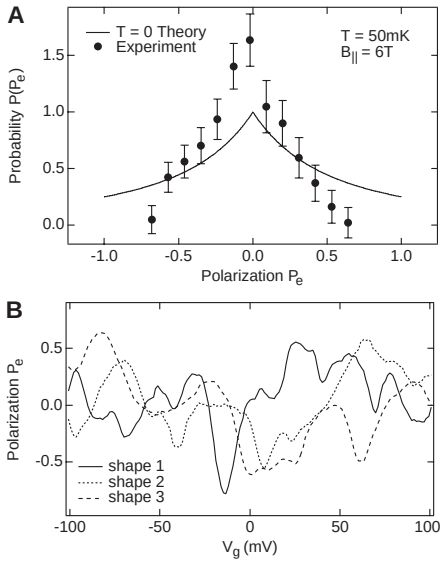

Fig. 4. (**A**) Experimental distribution of P_e over a dot-shape ensemble of ~200 independent samples, compared with random matrix theory. Statistics for P_e are based on the value $P_c = 0.7$ extracted for this device. (**B**) Examples of polarization fluctuations as a function of V_g for three different dot shapes.

spacing, zero temperature, and zero dephasing rate (*10*). This model gives a probability density for the spin polarization of current of the form $P(p) = 1/(1+|p|)^2$, with zero average and typical fluctuations (standard deviation) $\sigma(p) = 0.48$. Using the value of P_e determined above, the experimental value is $\sigma(p) = 0.27 \pm 0.06$.

It is not surprising that $\sigma(p)$ is overestimated by a zero-temperature theory. One may compare the reduction factor (relative to zero-temperature theory) for typical fluctuations of spin polarization with the analogous factor for conductance fluctuations. Conductance fluctuations measured simultaneously in the emitter dot gave $\sigma(g) = 0.21 \pm 0.02\ e^2/h$, which is 51% of the theoretical zero-temperature UCF value for single-mode leads (*8*), accounting for lifted spin degeneracy. This is consistent with the reduction factor $0.27/0.48 = 56\%$ observed for spin polarization. Despite the reduction factor, spin polarizations up to ~70% are readily obtained.

In summary, we have realized a quantum coherent spin filter based on interference in an open quantum dot, and we have measured its properties in a polarizer-analyzer geometry. Although the filtering properties of the dot require phase coherence within the dot, the resulting spin polarized current will remain polarized upon exiting the dot up to the spin relaxation time, which in practice may greatly exceed the phase coherence time. We find reasonable agreement between measured spin polarization statistics and a random matrix theory model. However, a fully developed theory of mesoscopic fluctuations of spin current is not yet in hand.

References and Notes

1. F. J. Jedema *et al.*, *Nature* **416**, 713 (2002).
2. P. R. Hammar, M. Johnson, *Phys. Rev. Lett.* **88**, 066806 (2002).
3. R. Fiederling *et al.*, *Nature* **402**, 787 (1999).
4. Y. Ohno *et al.*, *Nature* **402**, 790 (1999).
5. A. S. Sachrajda *et al.*, *Physica E* **10**, 493 (2001).
6. R. M. Potok *et al.*, *Phys. Rev. Lett.* **89**, 266602 (2002).
7. C. W. J. Beenakker, *Rev. Mod. Phys.* **69**, 731 (1997).
8. H. van Houten *et al.*, *Phys. Rev. B* **39**, 8556 (1989).
9. I. H. Chan *et al.*, *Phys. Rev. Lett.* **74**, 3876 (1995).
10. P. W. Brouwer, unpublished work.
11. We thank P. Brouwer for valuable contributions. This work was supported by the DARPA QuIST (Defense Advanced Research Projects Agency Quantum Information Science and Technology) Program and Army Research Office (ARO) under DAAD19-01-1-0659. J.A.F. acknowledges support from a Stanford Graduate Fellowship. R.M.P. acknowledges support as an ARO Graduate Research Fellow.

13 September 2002; accepted 23 December 2002

Zero-Mode Waveguides for Single-Molecule Analysis at High Concentrations

M. J. Levene,[1] J. Korlach,[1,2] S. W. Turner,[1]* M. Foquet,[1] H. G. Craighead,[1] W. W. Webb[1]†

Optical approaches for observing the dynamics of single molecules have required pico- to nanomolar concentrations of fluorophore in order to isolate individual molecules. However, many biologically relevant processes occur at micromolar ligand concentrations, necessitating a reduction in the conventional observation volume by three orders of magnitude. We show that arrays of zero-mode waveguides consisting of subwavelength holes in a metal film provide a simple and highly parallel means for studying single-molecule dynamics at micromolar concentrations with microsecond temporal resolution. We present observations of DNA polymerase activity as an example of the effectiveness of zero-mode waveguides for performing single-molecule experiments at high concentrations.

Data from a single molecule can reveal information about kinetic processes not normally accessible by ensemble measurements, such as variances in kinetic rates, memory effects, and lifetimes of transient intermediates (*1*, *2*). Single-molecule approaches to drug screening, mRNA expression profiling, single-nucleotide polymorphism detection and DNA sequencing may also have many advantages over current techniques (*3*–*5*). Common approaches to studying single molecules include fluorescence correlation spectroscopy (FCS) (*6*, *7*) and direct observation of sparse molecules using diffraction-limited optics (*8*, *9*). These approaches provide observation volumes on the order of 0.2 fl and therefore require pico- to nanomolar concentrations of fluorophore in order to isolate individual molecules in solution (*10*). However, many enzymes naturally work at much higher ligand concentrations, and their Michaelis constants are often in the micro- to millimolar range (*11*). Low concentrations of ligand can influence the mechanistic pathway of enzyme kinetics (e.g., by allosteric control or conformational relaxation) and alter the partitioning between multiple catalytic pathways, thus affecting turnover cycle histories and distributions (*12*). Working at biologically more relevant, micromolar concentrations requires reducing the observation volume by over three orders of magnitude.

In addition to requiring low concentrations of ligand, the temporal resolution of conventional approaches to single-molecule kinetics is often limited by the time it takes for molecules to diffuse out of the observation volume, usually on the order of several hundred microseconds. The temporal resolution and the upper limit of practicable concentrations would be greatly improved by reducing the effective observation volume.

Previous approaches include total internal reflection illumination, which can reduce the observation volume by a factor of 10 (*13*), and near-field scanning optical microscopy (NSOM), which achieves observation volumes with lateral dimensions on the order of 50 nm by illumination through a small aperture, usually terminating a tapered optical fiber (*14*). NSOM has been used to observe single molecules on a surface (*15*), but it suffers from unreliable probe manufacture and its complexity is not easily amenable to highly parallel implementations.

Concurrent to the development of single-molecule analytical techniques has been rapid progress in nanobiotechnology and efforts at

[1]Applied and Engineering Physics, [2]Graduate Program in Biochemistry, Molecular, and Cell Biology, Cornell University, Clark Hall, Ithaca, NY 14853, USA.

*Present address: Nanofluidics Incorporated, 17 Sheraton Drive, Ithaca, NY 14850, USA.

†To whom correspondence should be addressed. E-mail: www2@cornell.edu